Performance of inkjet-printed strain sensor based on graphene/silver nanoparticles hybrid conductive inks on polyvinyl alcohol substrate

Y. Z. N. Htwe[1] · I. N. Hidayah[1] · M. Mariatti[1]

Abstract

Recently, there have been considerable interests in strain sensors that are flexible and stretchable, due to their potential for use in wearable electronics applications. Herein, a facile approach has been employed to produce synergistic strain sensor, taking advantage of the salient properties of hybrid conductive inks produced from graphene and silver nanoparticles (AgNPs). The hybrid ink was inkjet-printed on a polyvinyl alcohol (PVA) substrate. The effect of factors such as amount of graphene, annealing time and printing cycle on the performance of the hybrid conductive ink was investigated. The results showed that an increase in the amount of graphene from 0.1 to 0.5 wt% produced about 90% enhancement in the electrical conductivity of the hybrid ink. However, the change in electrical conductivity values of the hybrid ink at 0.5 wt% and 0.7 wt% graphene content is negligible. On the other hand, it was observed that the electrical conductivity was notably influenced by the number of printing cycle, as well as the annealing time. Significantly, the sensitivity performance of the printed hybrid graphene/AgNPs strain sensor is higher than that of individual graphene and AgNPs printed strain sensors under the strain range up to 20%.

1 Introduction

There has been a recent advancement in the field of electronic devices and this had invariably expanded the scope of flexible electronics. In previous times, flexible electronics basically refer to the flexible, stretchable and foldable storage devices which are presently giving way to the more recent wearable and stretchable devices which are more advanced. Unfortunately, the operational scope of this set of recent electronic devices extends beyond the conventional material-based electronics which are significantly rigid [1]. Among the various wearable sensors, there has been a growing interest in the strain sensors in fields such as robotics, automotive and medicine. Particularly in medicine, they can be used for monitoring blood pressure, shape, force, strain and stress [2]. However, it has been observed that most of the conventionally fabricated strain sensors are generally too rigid with very low flexibility. This often results in undesirable separation between the sensor and the medium or substance that is being monitored [3]. Invariably, these devices could be damaged and as such, the results obtained from them are highly unreliable. As such, fabrication of flexible strain sensors through printing is being considered as a potential approach to overcome the peculiar shortcoming of sensors fabricated through the conventional methods. Interestingly, high mechanical flexibility at relatively low cost can be obtained from the printed flexible strain sensors [4].

Generally, wide strain-range materials with sufficient stability and sensitivity are required in flexible strain sensor applications. Therefore, nanomaterials are being exploited for strain sensor fabrication. Specifically, they are often incorporated in the sensitive part of the strain sensor, based on their impeccable performances which have been attributed to their very small size and dimension [5]. Several nanomaterials, such as carbon nanotube, graphene, AgNPs and silver nanowires, have all been widely investigated for the fabrication of flexible strain sensors. This is mainly associated with their high conductivity and desirable mechanical properties. In this group of materials, the outstanding electrical and mechanical properties of graphene and silver nanoparticles (AgNPs) make them particularly interesting, with great prospects for development [6].

Graphene is a two-dimensional (2D) material, which basically comprises a honeycomb-lattice of linked carbon

✉ M. Mariatti
mariatti@usm.my

1   School of Materials and Mineral Resources Engineering, University Sains Malaysia, 14300, Engineering Campus, Nibong Tebal, Pulau Pinang, Malaysia

atoms. Most of the research interest in graphene is generally associated with its peculiar features such as great aspect ratio, large surface area, highly mobile electron, desirable piezoresistivity and sufficient mechanical flexibility [7]. Significantly, graphene can withstand high mechanical strains without significant electrical degradation. This is associated with its high flexibility and this makes it an ideal candidate for the fabrication of sensors and other electronic devices where highly stretch ability and good flexibility are required [8]. On the other hand, AgNPs have also been observed to exhibit good physical and chemical properties. In fact, based on the excellent performance of AgNPs in electrical fields, they can be used as a viable choice for the sensitive parts of strain sensors. It has been reported that hybrid graphene and AgNP structures perform better compared to individual structures based on either graphene or silver nanoparticles. Specifically, this hybrid material possesses significantly better properties, due to the reduced aggregation achieved through the intercalation of nanoparticles between the graphene sheets. This invariably presents novel synergistic performance [9].

In recent years, conductive inks have gained more popularity in the field of printed electronics. However, the type of solvent used would influence the ability of the conductive ink to attain the desired viscosity required for printing [10]. As such, the features of the ink solutions play a significant role in determining the mechanical and electrical performance of the conductive material. Generally, it is required that the conductive ink should have good stability against precipitation in order to ensure steady performance and consistent conductive patterns [11]. Therefore, specific viscosity and surface tension are among the notable requirements for the printability of conductive inks, using the available facilities. This is because an incompatible or poorly prepared ink solution may result in failure of the printing process or the printing devices and this could affect the quality of the conductive traces. On the other hand, low volatilising temperature, coupled with good adhesion properties, is important for widespread use of the inks on the substrates. This would help to ensure that the printed item is flexible and stretchable [12]. Considering the very many advantages of soft strain sensors, various soft substrates have been investigated by different researchers. Particularly, polyvinyl alcohol (PVA) fulfils the requirements of soft substrates, and it is therefore suitable to be used as the flexible substrate in electronic skin sensor applications [13].

It is well known that parameters such as stress and strain can be effectively measured using a strain gauge which is basically a sensor [14]. Therefore, in strain sensor applications, the strain sensor data are generally assessed based on the gauge factor (GF) which is considered as the standard for quantifying the piezoresistive sensitivity.

The GF can be simply described as the ratio of the relative change in electrical resistance with respect to the unit change in length.

Herein, strain sensor was fabricated from hybrid conductive ink produced from graphene and AgNPs, which was printed on a PVA substrate. Based on extensive literature review, it was observed that there are limited studies on the property evaluate of strain sensors fabricated by combination of graphene/AgNPs ink on PVA substrate. Particularly, the influence of the amount (wt%) of graphene on the properties of the hybrid conductive ink such as morphology, surface wettability, stability and electrical conductivity was investigated. In addition, the effect of varying printing cycles, as well as annealing time on the electrical conductivity of the printed film, was studied. To assess the performance of graphene/AgNPs hybrid conductive ink as a strain sensor, the substrate-printed ink was stretched at different strains, such as 5, 10 and 20%. Then the variation in resistivity of graphene, AgNPs and graphene and AgNPs hybrid ink with respect to was measured and compared the sensistivity.

2 Experimental section

2.1 Materials

The important chemicals used in this study are polyvinyl alcohol (PVA), dimethylformamide (DMF), glycerol (G) and ethylene glycol (EG). These chemicals were procured from Sigma-Aldrich. The PVA was supplied in powder form and the other chemicals were used mainly used as chemical solvents in the conductive ink preparation. The PVA solution was prepared and cast to form a thin film which was used as a substrate.

2.2 Methodology

The graphene used in this study was synthesised via the electrochemical exfoliation method, as reported in our previous work [15]. Likewise, the AgNPs were synthesised through a chemical reduction method as described previously [16]. The hybrid conductive inks were formulated by incorporating different amounts (wt%) of graphene (0.1, 0.3, 0.5, 0.7 wt%), while the amount of silver nanoparticles was fixed at 0.5 wt%. The ratio of DMF, EG and G used as the solvent is DMF:EG:G = 50:45:5. Prior to the printing, the formulation was first placed in a centrifuge running at 2000 rpm for a period of about 15 min. Thereafter, the ink was substrate-printed on the PVA with the help of a Canon PIXMA E 510 inkjet printer. Then, the print was annealed at 80 °C for different periods of time such as 10, 20 and 30 min.

2.3 Material characterisation

The viscosity of the produced inks was measured by a PCE-RVI 6 Kerbs Stormer viscosity meter. On the other hand, the wavelength and intensities of the visible light and near-ultraviolet absorption of the graphene- and AgNP-based inks of were measured in a Perkin Elmer UV–Vis spectrometer (Lambda 35). A ZEM 3600 zeta potential equipment (Malvern nano series) was used to measure the zeta potential, while a contact angle goniometer was used to assess the contact angle and wetting properties of the inks. On the other hand, the surface morphology of the conductive films produced was observed on a Supra 35 VP field emission scanning electron microscope (FESEM). In addition, resistance measurement was used to investigate the electrical conductivity of the conductive films. Notably, the resistance was measured during a tensile test. Furthermore, a FLUKE 115 digital multimeter was used to check the relative change in resistance of the sensors. The gauge factor was obtained as the slope of the plot of resistance against strain and was found to increase as the maximum strain increased. The gauge factor is simply defined as the ratio of the relative resistance change per unit strain as presented in the equation below:

$$\text{Gauge factor} = \frac{\Delta R/R_o}{\Delta L/L_o}, \tag{1}$$

where ΔR represents the relative change in resistance under deformation, while R_o, L_o and ΔL represents the initial strain resistance (%), the initial sensor length and the elongation of the specimen, respectively.

3 Results and discussion

It is well known that in conductive ink technology, the ink viscosity plays an important role. The viscosity of the graphene/AgNPs hybrid conductive inks with various contents of graphene (0.1, 0.3, 0.5, 0.7 wt%) is presented in Table 1. It was found that the viscosity values for all inks range between (9–14) cp, which indicates that all the hybrid

Table 1 Zeta potential and contact angle values of graphene and AgNPs hybrid conductive inks with different contents of graphene loading

Contents of graphene (wt%)	Viscosity (cP)	Zeta potential (mV)	Contact angle (°)
0.1	9	− 39	19
0.3	10	− 40	16
0.5	12	− 43	15
0.7	14	− 43	15

conductive inks are suitable for inkjet printing. It has been reported in the literature that the inkjet printing required less viscous inks and a viscosity range of 8–15 cp is sufficient for conductive inks intended to be inkjet-printed [17]. With this viscosity range, the flow of the ink through the nozzle would be enhanced, without issues bordering on leaking, drying out or coagulation.

The UV–Vis spectra of graphene/AgNPs hybrid conductive inks with various graphene contents were recorded over a wavelength range of 300–800 nm. As can be seen in the UV–Vis spectra illustrated in Fig. 1, the absorption spectrum of graphene is observed around 278 nm. This may be accrued to the π–π* transition of the C–C aromatic ring present in the graphene conductive ink. After adding AgNPs into graphene, absorption peaks should reflect the presence of AgNPs and this is evident in the adsorption peak at 417 nm. Notably, this adsorption represents the surface plasmon resonance of AgNPs. Significantly, the peak position of graphene in the hybrid inks moved to 265 nm which represents a blue shift of about 13 nm compared to ink based on graphene alone. This notable blue shift is due to the interactive transfer of charges AgNPs and graphene. It is noteworthy that the UV–Vis absorbance peaks observed for the graphene/AgNPs hybrid conductive inks in this study align with what was previously reported in literature by Zhang et al. [18], in a similar study on Ag/RGO conductive ink.

Stability of the hybrid inks in DMF:EG:G = 50:45:5 solution was investigated through UV–Vis analysis. The UV–Vis spectra of the graphene and AgNPs hybrid conductive inks with various contents of graphene (0.1, 0.3, 0.5, 0.7 wt%) are illustrated in Fig. 2. It should be noted that the spectra were taken immediately after sonication when the conductive inks were freshly prepared, and after a standing period
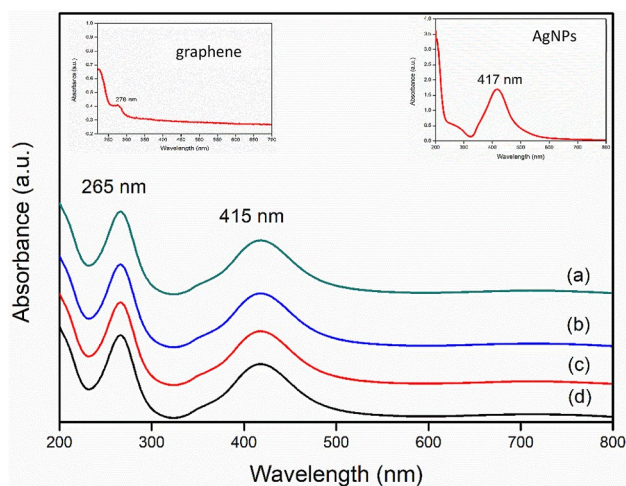

Fig. 1 UV–Vis spectra of graphene, AgNPs hybrid conductive ink with graphene content of (a) 0.1 wt%, (b) 0.3 wt%, (c) 0.5 wt% and (d) 0.7 wt%
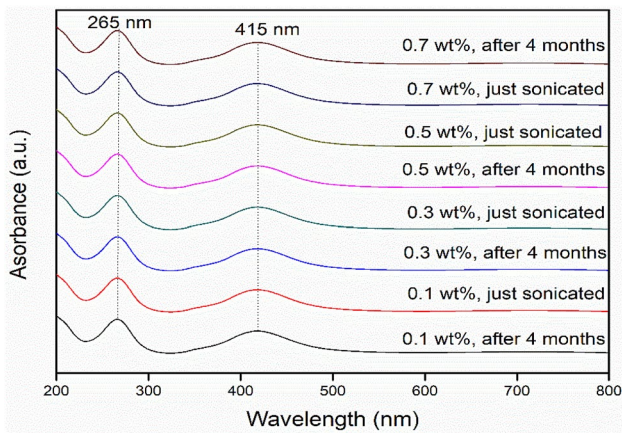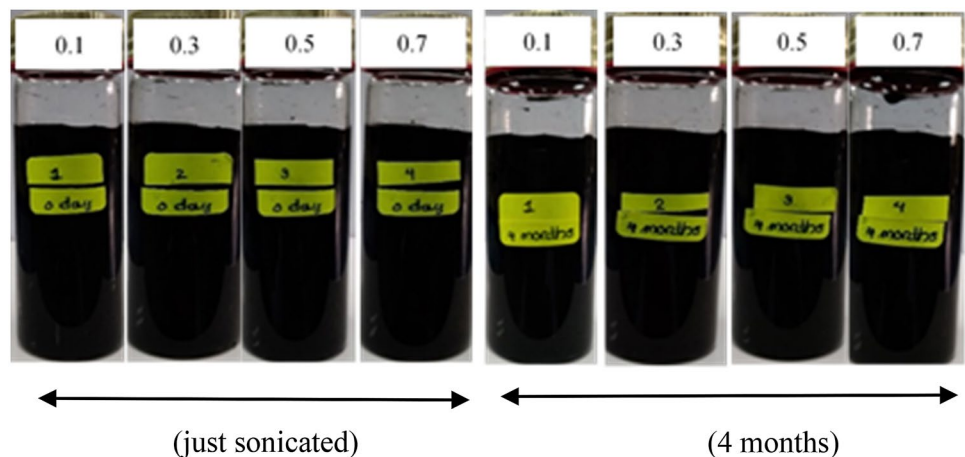
Fig. 2 UV–Vis spectra of graphene and AgNPs hybrid conductive inks with graphene contents of 0.1, 0.3, 0.5 and 0.7 wt% at different storage times

of 4 months after sonication, respectively. It can be observed that there is no significant change in the UV–Vis absorbance peak of the hybrid inks even after being allowed to stand for 4 months. This is an indication that all the graphene/AgNPs hybrid conductive inks are stable up to 4 months. Similar observation was also reported previously in a study on preparation of flexible electronics from hybrid conductive inks produced from Ag and RGO [18].

Figure 3 shows the visual inspection of graphene/AgNPs as conductive inks at various contents of graphene loading. No obvious sedimentation was observed and the dispersion appears to be homogeneous, but with a dark black appearance distributed in the ink after they have been allowed to stand for 4 months. This suggests that the conductive inks produced from different formulations of graphene/AgNPs hybrid were very stable, and this observation aligns with the result obtained from the UV–Vis analysis. The zeta potential is notable for its ability to describe the surface of

nanoparticles, thereby predicting the potential long-term stability of the conductive ink. The zeta potential and contact angle values of the hybrid inks produced here are summarised in Table 1. The zeta potential values indicate that all the different graphene loadings incorporated in the hybrid conductive inks support good stability. This is because literature has confirmed that a dispersion can be considered to exhibit good stability if the zeta potential value > 30 mV or < − 30 mV [17].

One of the factors that could influence a printing process is the layer of substrate under the printed layer because the wettability of the substrate is highly dependent on its surface energy. The pendant images of a conductive ink, dispensed on the PVA substrate through the needle of the goniometer, are shown in Fig. 4. The contact angel values presented in Table 1 show that the contact angle values of all the hybrid conductive inks are below 19° which indicates that all the hybrid conductive inks exhibit good wettability regardless of the amount of graphene incorporated. Saidina et al. [19] reported that contact angle less than 90° relates to better wettability of a PVA printed ink. Figure 5 shows the PVA printed hybrid graphene/AgNPs conductive inks with different amounts (wt%) of graphene and varying printing cycles.
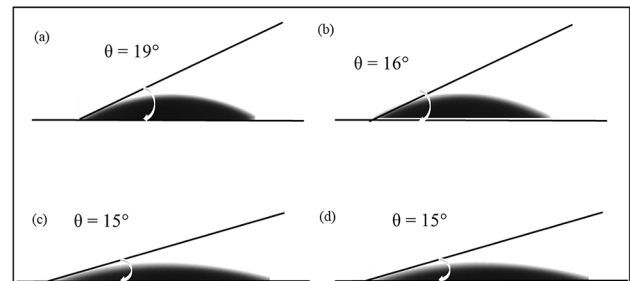

Fig. 4 The droplet of graphene and AgNPs as conductive inks on the PVA substrate with contents of graphene loading **a** 0.1 wt%, **b** 0.3 wt%, **c** 0.5 wt% and **d** 0.7 wt%
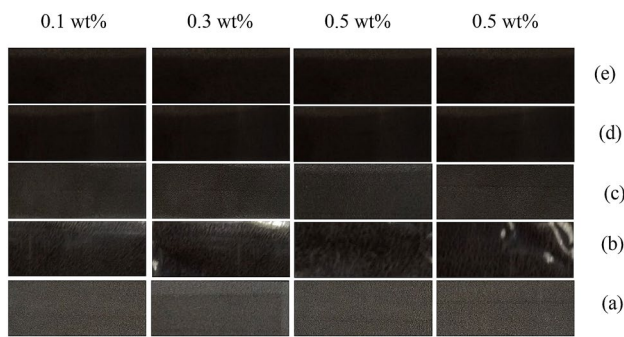
Fig. 3 Photographs of graphene and AgNPs hybrid conductive ink contents of graphene loading (1) 0.1 wt%, (2) 0.3 wt%, (3) 0.5 wt% and (4) 0.7 wt%

(just sonicated)   (4 months)

Fig. 5 Printed graphene and AgNPs as conductive inks on PVA substrate with different graphene contents using different numbers of printing cycles (a) 1 time, (b) 2 times, (c) 3 times, (d) 4 times and (e) 5 times

It can be seen in the figure that as the number of the printing cycle increased, there is a concurrent increase in the number of ridges with a progressively darkening of the print colour. It was reported by Dennueulin et al. [20] that increased in the number of printing layers caused the connection between the conductive films to increase which resulted in a decrease in the sheet resistance.

The values of electrical conductivity recorded for the PVA printed hybrid inks containing different wt% graphene loadings and printed at different printing cycles are presented in Fig. 6a. It was observed that increase in the graphene loading from 0.1 wt% to 0.5 wt% increased the conductivity of the ink printed at one cycle from 0. 1028 S m^{-1} to 0.1962 S m^{-1}. This can be attributed to the increasing amount of graphene in the printed pattern. This is because at low graphene loading, the amount of graphene might be too low to form the conductive network pattern which will invariably result in poor conductivity. On the other hand, there would be no further increase in conductivity if the total amount of graphene flakes available has been fully contacted with AgNPs. This is the case when the graphene loading was 0.5 wt%. As such, it can be seen in Fig. 6 that no significant changes in the electrical conductivity values when the graphene loading was increased from 0.5 to 0.7 wt% of graphene were found. It is believed that conductive filler loading at 0.5 wt% to 0.7 wt% are above the percolation threshold. The result is in accordance with the findings reported in previous works [21, 22]. Theoretically, above the percolation threshold, multiple electron paths already exist in polymer composites; hence, the electrical conductivity of the composites reaches a saturation state. This result can be explained schematically by referring to the illustration of graphene/AgNPs hybrid with low and high graphene loadings as presented in Fig. 6b. At low loading (0.1 wt%), conductive fillers are not contacted well everywhere; there are narrow gaps separating them which prevent the continuous linkage and hence decrease the current carrier throughout the composite. When the fillers have reached a critical loading (0.5 wt%), the two hybrid materials are attached to each other. With further increase of filler up to 0.7 wt%, only a small increase in conductive path could form, hence leading to a relatively small increase in conductivity. Therefore, 0.5 wt% of graphene loading of graphene/AgNPs hybrid conductive inks was identified as a sufficient amount of graphene in the hybrid ink. The results were supported by the stability value, as shown by the zeta potential and contact angle.

Figure 7 shows the pattern morphologies of 0.5 wt% of graphene in graphene/AgNPs hybrid, printed at 1, 3 and 5 times printing cycles. In Fig. 7a, there were many gaps showing pore structures of 1 time printing cycles of the graphene/AgNPs hybrid conductive pattern. In addition, few of the AgNPs agglomerated and some wrinkled structures were also observed on the pattern. When the printing cycles increased to three times, the graphene flakes still maintained the wrinkled flat structures, as observed in Fig. 7b. In Fig. 7c, it is evident that less pore and gap structures exist with the increase in printing cycles to 5 times. The increase in number of printing layer from 1 to 5 times helped to facilitate improved continuity in the printed patterns.

The electrical conductivity of the hybrid inks obtained from 0.5 wt% amount of graphene and printed for 5 printing cycles is presented in Fig. 8. The ink was annealed at 80 °C for varying annealing durations (5, 10, 15, 20 and 30 min). As shown in Fig. 8, an increase in the annealing time from 0 to 30 min produced a sharp increase in the electrical conductivity from 0.3545 S m^{-1} to 2.1517 S m^{-1}. It is observed that the electrical conductivity was significantly influenced by the annealing temperature, due to changes in the printed pattern. As such, increasing the annealing time could help to slightly melt the particles that can contribute to the compactness of the particles, thus forming the conductive network as reported in the literature [23]. Increase in conductive trend of conductive ink with annealing time was also reported in the previous works [24, 25]. However, it should be reiterated here that high annealing temperature is not suitable for flexible substrate. Therefore, in our study, the low annealing temperature was used in order to prevent degradation of the PVA substrate.

The morphologies of 0.5 wt% graphene/0.5 wt% AgNPs hybrid conductive inks for 5 times printed cycles, before and

Fig. 6 **a** Electrical conductivity of graphene and AgNPs hybrid conductive inks printed on PVA substrate with different formulations and different printing layers. **b** Low content and high content of electrical conductive electron flow for graphene/ AgNPs hybrid conductive ink pattern
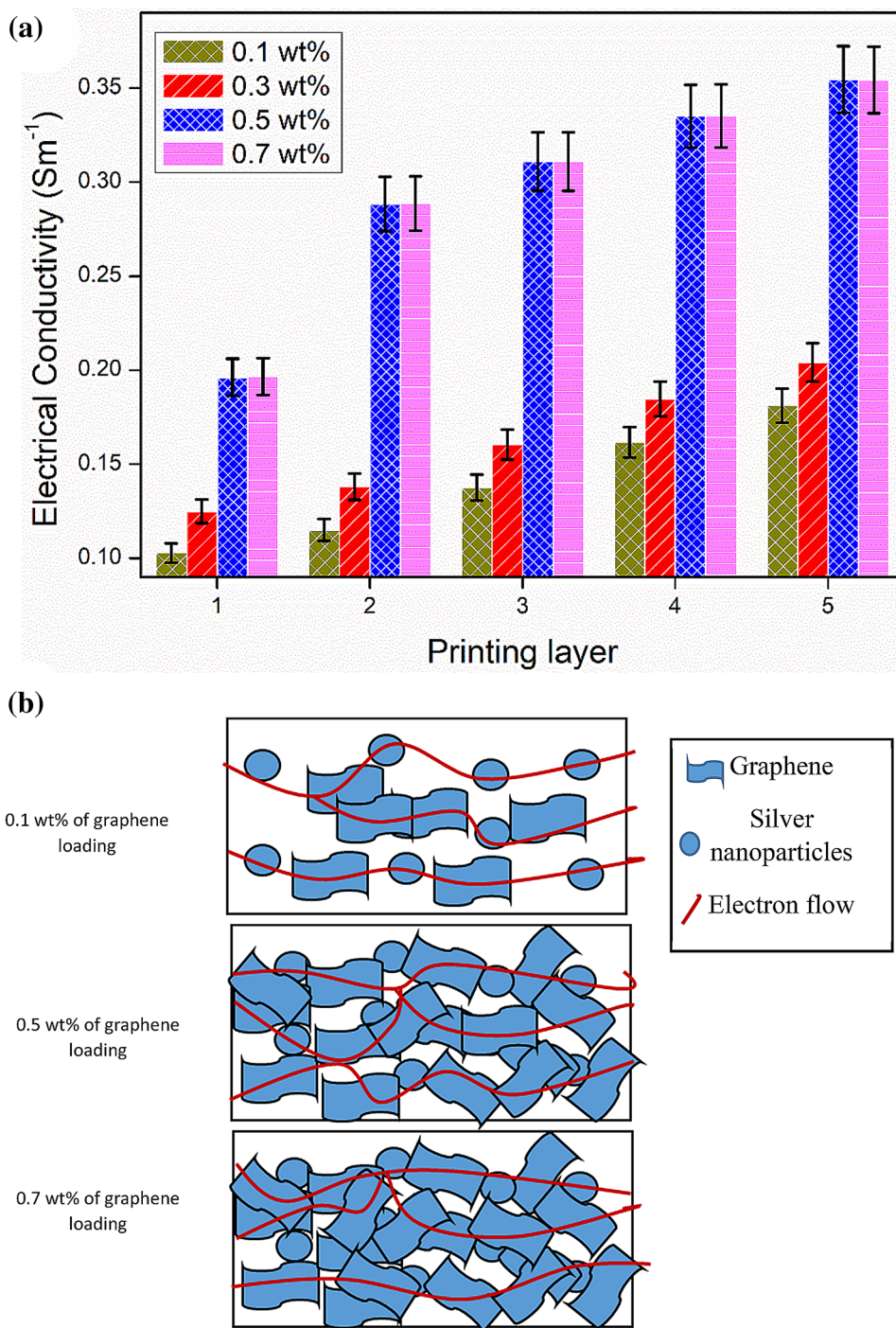
after annealed at 80 °C at 30 min, are shown in Fig. 8. From the microstructure, it is observed that less pore and some gaps were found in the conductive pattern before annealing. However, an increase in the annealing time to 30 min helped to facilitate gradual formation of the conductive pattern due to increased contacts. In addition, the conductive pattern was uniformed and no gap and obvious pores are observed. This result was confirmed by the highest electrical conductivity

Fig. 7 Morphologies of graphene and AgNPs hybrid conductive inks with 0.5 wt% graphene loading printed on PVA substrates at **a** 1 time, **b** 3 times, and **c** 5 times printing cycles at magnifications of (i) 10 KX and (ii) 30 KX
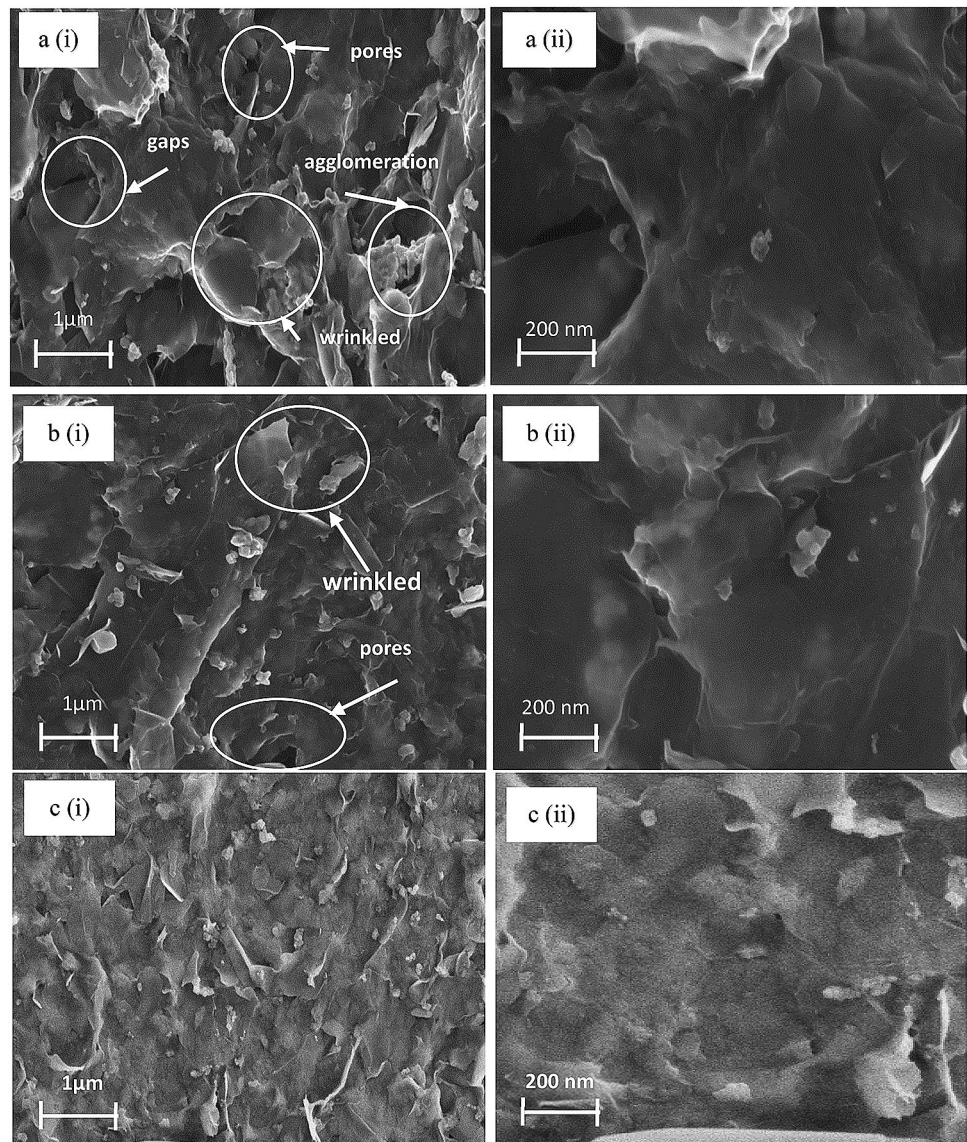

values shown by graphene/AgNPs hybrid conductive ink, printed 5 times printing cycles after annealed at 80 °C for 30 min. Based on the analysis of the results, 0.5 wt% graphene/0.5 wt% AgNPs hybrid conductive inks printed for 5 times printing cycles and annealed at 80 °C at 30 min were chosen to be used in the formulations of stretchable strain sensor.

The electromechanical properties of conductive inks based on graphene, AgNPs and graphene/AgNPs hybrid printed strain sensor were characterised using tensile test.

The resistance of the strain sensors at different strains (5, 10 and 20%) are shown in Fig. 9a–c. Similar resistance trend was shown by these three strain sensors; however, graphene/AgNPs hybrid strain sensor exhibit lower resistance if compared to those graphene and AgNPs sensors. A good linearity is observed for all strain sensors, with the best linearity shown by graphene/AgNPs hybrid sensor. According to Shengbo et al. [26], it is required of a strain sensor to exhibit good linearity. This would make it easier to obtain the strain rate as long as the resistance change is known.

Fig. 8 Electrical conductivity of 0.5 wt% graphene and 0.5 wt% AgNPs conductive inks printed on PVA substrates with 5 times printing layers annealed at 80 °C for different time periods (5 to 30 min). Morphology of the ink is shown in the circle.
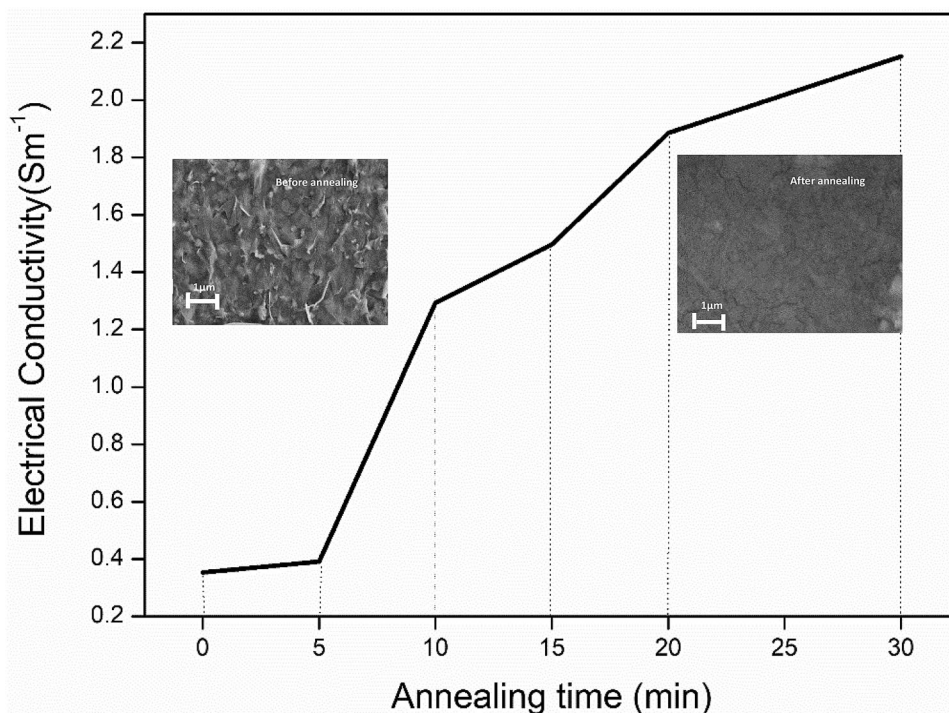
In other words, good linearity is an indication that stretching of the sensor would produce only slight changes in the resistance.

The difference in the relative resistance change ratio between the stretching and releasing process is also an important factor to evaluate the performance of the strain sensor. Figure 10a–c illustrates the hysteresis curves for graphene, AgNPs and graphene/AgNPs hybrid printed strain sensor with different strain ranges (5, 10 and 20%). In the figure, small hysteresis was observed for graphene and AgNPs strain sensors during 5% tensile strain. However, very small hysteresis was observed in the response of the graphene/AgNPs hybrid strain sensor. The same trend was observed for 10% and 20% strain ranges, where small hysteresis was observed for graphene/AgNPs hybrid strain sensors, compared to that of graphene and AgNPs strain sensors. Based on the hysteresis curves in Fig. 10, it is found that the hysteresis performance of graphene/AgNPs hybrid strain sensors is much better than only graphene and AgNPs strain sensors. This is because the graphene flakes have a tendency to align, and the distance between the flake shape of graphene and spherical shape of AgNPs is still closer and allows electrons to travel from one point to another. It was shown in the schematic diagram in Fig. 11 that the hybrid of graphene and AgNPs exhibited added advantages compared to the ink based on single nanoparticles.

The performance of graphene, AgNPs and graphene/AgNPs as printed strain sensors is listed in Table 2. It is observed that the gauge factor of printed AgNPs strain sensor is lower than that of graphene and graphene/AgNPs, as printed strain sensors. This result aligns with what was previously reported by Shengbo et al. [26] on nanoparticle-based wearable strain sensor. They reported AgNPs cannot make a conductive network during stretching. This is due to the tendency for graphene flakes to align, and the close similarity between the flake shape of graphene and spherical shape of AgNPs. This would permit the electrons to move from one point to another. It was shown in the schematic diagram in Fig. 11 that the hybrid of graphene and AgNPs exhibited added advantages compared to the ink based on single nanoparticles. With the increase of the applied strain, the resistance changed because of the variation of distance of neighbouring nanoparticles.

The results are compared with the data presented in the previous work. It can be observed that most of the strain sensor used polydimethylsiloxane (PDMS) substrate. The AgNPs-based sensors show low sensitivity (GF) because of their sensing mechanism. This is because the mechanical separation of AgNPs during stretching would encourage drastic change of relative resistance, leading to electrical disconnection above the specific level of strain
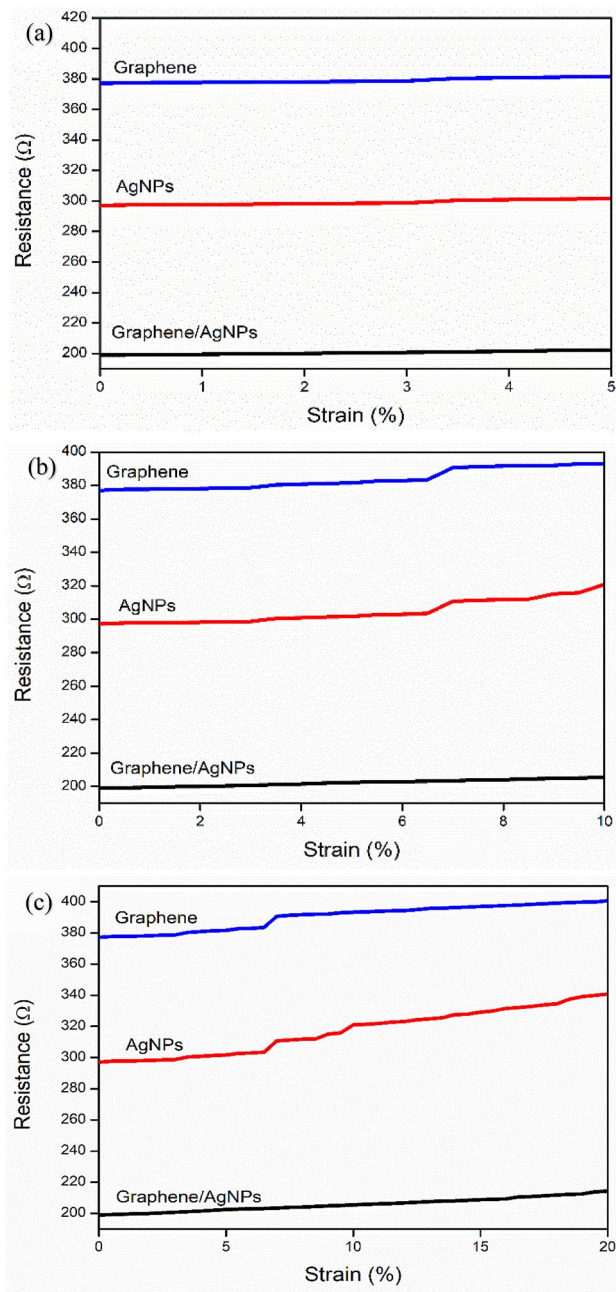
Fig. 9 Resistance and strain range of graphene, AgNPs and graphene/AgNPs hybrid printed strain sensors with different strain ranges **a** 5%, **b** 10%, **c** 20%

Fig. 10 Hysteresis curve for graphene, AgNPs and graphene/AgNPs hybrid printed strain sensors with different strain ranges **a** 5%, **b** 10%, **c** 20%

[27]. On the other hand, graphene-based stain sensors show high sensitivity but large strain range. The graphene, which is electrically conductive and combined in the highly stretchable PDMS, enables the production of large stretchable strain sensor [27]. Based on the study, the sensitivity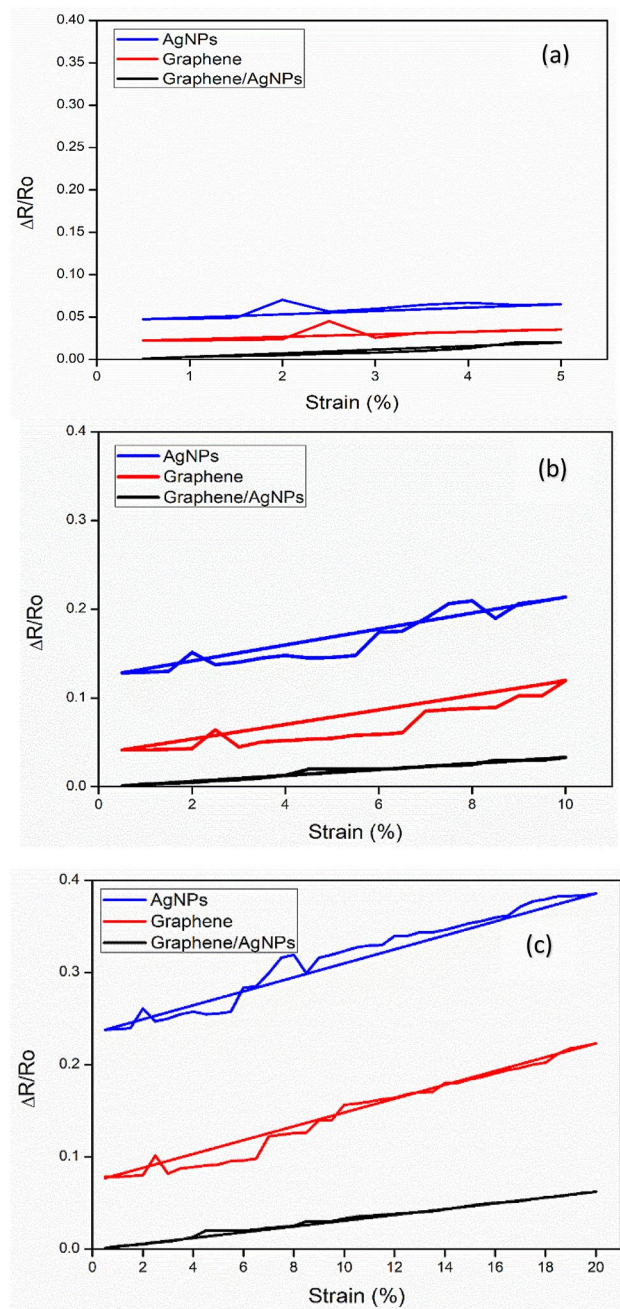 of the strain sensor based on graphene/AgNPs hybrid is higher and the strain ranges are lower and comparable to those reported by the previous work.
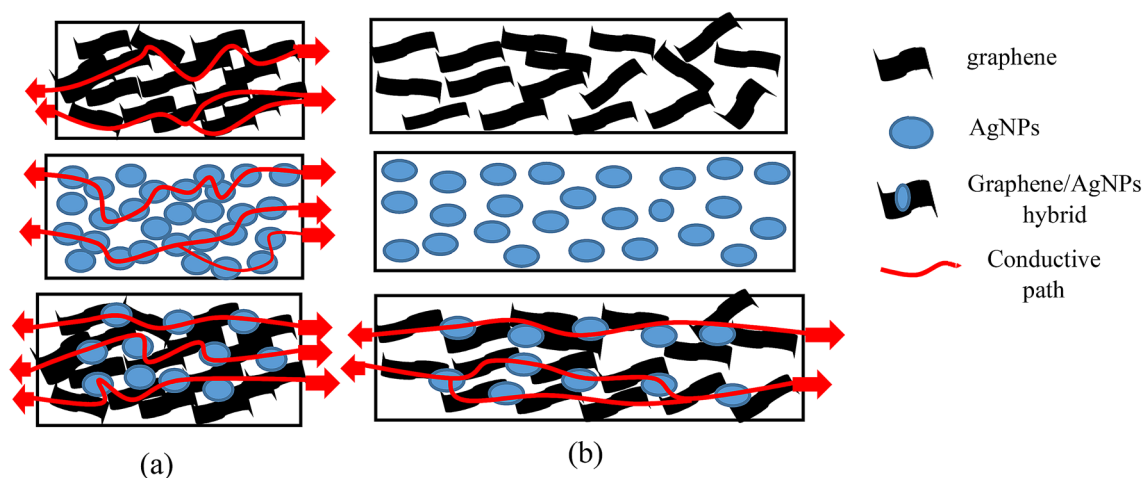
Fig. 11 Schematic illustration of graphene, AgNPs and graphene/AgNPs hybrid conductive film **a** before stretching and **b** after stretching

Table 2 Comparison between gauge factor and strain ranges with different types of strain sensor from literature and present study

Materials	Gauge factor	Strain range (%)	References
Graphene	97	0–20	Present study
AgNPs	76	0–20	Present study
Graphene/AgNPs	149	0–20	Present study
AgNPs/PDMS	14	0–70	[28]
AgNPs/PDMS	2.05	0–20	[29]
Graphene/PDMS	42.2	0–20	[28]
Graphene/PDMS	25	0–35	[30]
AgNPs/CNT/PDMS	39.8	0–100	[31]

4 Conclusions

This study reports the production of hybrid conductive inks from graphene and AgNPs with different concentrations of graphene. The increasing stability and wetting properties with increasing concentrations of graphene loading were observed based on the measurement performed using zeta potential and contact angle study. Based on the electrical conductivity measurement, the combination of 0.5 wt% graphene in 0.5 wt% AgNPs exhibits the highest conductivity values compared to other conductive inks. Notably, increasing the number of printing cycles and annealing time resulted in increasing electrical conductivity. This was attributed to the improved continuity of the printed patterns as the printing cycle and annealing time were increased. The 0.5 wt% graphene/0.5 wt% AgNPs hybrid-based strain sensor shows high gauge factor and high sensitivity compared to strain sensors based on either graphene or and AgNPs alone.

Therefore, it can be inferred that the hybrid graphene/AgNP conductive ink is suitable for use as a strain sensor.

References

1. J. Wang, W. Zhang, Q. Yin, B. Yin, H. Jia, Highly sensitive and flexible strain sensors based on natural rubber/graphene foam composites: the role of pore sizes of graphene foam. J. Mater. Sci.: Mater. Electron. **31**(1), 125–133 (2020)
2. X.M. Zhang, X.L. Yang, K.Y. Wang, Conductive graphene/polydimethylsiloxane nanocomposites for flexible strain sensors. J. Mater. Sci.: Mater. Electron. **30**(21), 19319–19324 (2019)
3. C. Deng, L. Pan, R. Cui, C. Li, J. Qin, Wearable strain sensor made of carbonized cotton cloth. J. Mater. Sci.: Mater. Electron. **28**(4), 3535–3541 (2017)
4. A.M. Gaikwad, D.A. Steingart, T.N. Nga, D.E. Schwartz, G.L. Whiting, A flexible high potential printed battery for powering printed electronics . Appl Phys. Lett. **102**(23), 104–101 (2013)
5. S.H. Eom, S. Lim, RF stretchable sensor using flexible substrate and eutectic gallium-indium. In *Proceedings of the Antennas and Propagation (ISAP), International Symposium on* IEEE, pp. 996–997 (2016)
6. H. Dai, E.T. Thostenson, T. Schumacher, Processing and characterization of a novel distributed strain sensor using carbon nanotube-based nonwoven composite. Sensors **15**(7), 17728–17747 (2015)
7. K. Karimi, E. Jabari, E. Toyserkani, P. Lee-Sullivan, Highly conductive graphene paper for flexible electronics applications. J. Mater. Sci.: Mater. Electron. **29**(3), 2537–2549 (2018)
8. M. Goosey, A short introduction to graphene and its potential interconnect applications. Circuit World **38**(2), 83–86 (2012)

9. Z. Zhong, X. Gong, L. Wang, G. Bai, H. Wei, W. Yang, A facile way for fabrication of silver nanoparticle decorated graphene composites. Mater. Chem. Phys. **241**, 122344 (2020)

10. D. Deng, S. Feng, M. Shi, C. Huang, In situ preparation of silver nanoparticles decorated graphene conductive ink for inkjet printing. J. Mater. Sci.: Mater. Electron. **28**(20), 15411–15417 (2017)

11. F. Miao, S. Majee, M. Song, J. Zhao, S.L. Zhang, S. L, Z.B. Zhang, Inkjet printing of electrochemically-exfoliated graphene nano-platelets. Synth. Met. **220**, 318–322 (2016)

12. T.S. Tran, N.K. Dutta, C.N. R, Graphene inks for printed flexible electronics: Graphene dispersions, ink formulations, printing techniques and applications. Adv Colloid Interfac **261**, 41–61 (2018)

13. M.R. Ammar, G. Legeay, A. Bulou, J.F. Bardeau, Physical and chemical treatments of surface for improved adhesion of PVA Coating. In *Proceedings of the Le Congrès National de la Recherche des IUT*, pp. 1–6 (2008)

14. Y. Wan, Y. Wang, C.F. Guo, Recent progresses on flexible tactile sensors. Mater. Today Phy. **1**, 61–73 (2017)

15. Y.Z.N. Htwe, W.S. Chow, Y. Suda, A.A. Thant, M. Mariatti, Effect of electrolytes and sonication times on the formation of graphene using an electrochemical exfoliation process. Appl. Surf. Sci. **469**, 951–961 (2019)

16. Y.Z.N. Htwe, W.S. Chow, Y. Suda, A.A. Thant, M. Mariatti, Properties enhancement of graphene and chemical reduction silver nanoparticles conductive inks printed on polyvinyl alcohol (PVA) substrate. Synth. Met. **256**, 116–120 (2019)

17. W. Zhang, E. Bi, M. Li, L. Gao, Synthesis of Ag/RGO composite as effective conductive ink filler for flexible inkjet printing electronics. Colloids Surf. A **490**, 232–240 (2016)

18. A. Kamyshny, J. Steinke, S. Magdassi, Metal-based inkjet inks for printed electronics. J. Appl. Phys. **4**(1), 19–36 (2011)

19. D.S. Saidina, S.A. Zubir, S. Fontana, C. Hérold, M. Mariatti, Synthesis and characterization of graphene-based inks for spray-coating applications. J. Electron. Mater. **48**, 5757–5770 (2019)

20. A. Denneulin, J. Bras, A. Blayo, B. Khelifi, F. Roussel-Dherbey, C. Neuman, The influence of carbon nanotubes in inkjet printing of conductive polymer suspensions. Nanotechnology **20**(38), 385–701 (2009)

21. G. Suriati, M. Mariatti, A. Azizan, A effects of filler shape and size on the properties of silver filled epoxy composite for electronic applications. J. Mater. Sci.: Mater. Electron. **22**(1), 56–63 (2009)

22. A.J. Marsden, D.G. Papageorgiou, C. Vallés, A. Liscio, V. Palermo, M.A. Bissett, I.A. Kinloch, Electrical percolation in graphene–polymer composites. 2D Mater. **5**(3), 032003 (2018)

23. Y. Gao, W. Shi, W. Wang, Y. Leng, Y. Zhao, Inkjet printing patterns of highly conductive pristine graphene on flexible substrates. Ind. Eng. Chem. Res. **53**(43), 16777–16784 (2014)

24. J. Li, X. Zhang, X. Liu, Q. Liang, G. Liao, Z. Tang, T. Shi, Conductivity and foldability enhancement of Ag patterns formed by PVAc modified Ag complex inks with low-temperature and rapid sintering. Mater. Des. **185**, 108255 (2020)

25. N. Karim, S. Afroj, S. Tan, K.S. Novoselov, S.G. Yeates, All inkjet-printed graphene-silver composite ink on textiles for highly conductive wearable electronics applications. Sci. Rep. **9**(1), 1–10 (2019)

26. S. Shengbo, L. Lihua, J. Aoqun, D. Qianqian, J. Jianlong, Z. Qiang, Z. Wendong, Highly sensitive wearable strain sensor based on silver nanowires and nanoparticles. Nanotechnology **29**(25), 255–202 (2018)

27. H. Lee, B. Seong, H. Moon, D. Byun, Directly printed stretchable strain sensor based on ring and diamond shaped silver nanowire electrodes. RSC Adv. **5**(36), 28379–28384 (2015)

28. S. Chun, Y. Choi, W. Park, All-graphene strain sensor on soft substrate. Carbon **116**, 753–759 (2017)

29. M. Amjadi, A. Pichitpajongkit, S. Lee, S. Ryu, S.I. Park, Highly stretchable and sensitive strain sensor based on silver nanowire–elastomer nanocomposite. ACS Nano **8**(5), 5154–5163 (2014)

30. Y. Liu, D. Zhang, K. Wang, Y. Liu, Y. Shang, A novel strain sensor based on graphene composite films with layered structure. Compos. Part A Appl. Sci. Manuf. **80**, 95–103 (2016)

31. S. Zhang, H. Zhang, G. Yao, F. Liao, M. Gao, Z. Huang, Y. Lin, Highly stretchable, sensitive, and flexible strain sensors based on silver nanoparticles/carbon nanotubes composites. J. Alloys Compd. **652**, 48–54 (2015)